UNIVERSITY OF
BATH

University of Bath

PARP10 INFLUENCES THE PROLIFERATION OF COLORECTAL CARCINOMA CELLS, A PRELIMINARY STUDY

ChengFang Wu,[1#] Ming Xiao,[1#] YaLan Wang,[1]* Michael D. Threadgill,[2] Ming Li,[1] Yi Tang[1] , Xiao Lin[1], Lian Yang[1], QingShu Li[1], Xian Li[1]

[1]*Department of Pathology, Molecular Medicine and Cancer Research Center, Chongqing Medical University, Chongqing, China*

[2] *Department of Pharmacy & Pharmacology, University of Bath, Bath BA2 7AY, United Kingdom.*

*e-mail: wangyalan@cqmu.edu.cn

PARP10 is an intracellular mono-ADP ribosyltransferase and recent reports suggest that it regulates proliferation of some cell types. However, its effect on the proliferation of colorectal carcinoma cells has not yet been systematically reported. We explored the influence of PARP10 on the proliferation of several colorectal carcinoma cell types and carried out initial studies on the underlying mechanisms. Inhibition of the enzymatic activity of PARP10 led to significantly decreases in proliferative ability in LoVo cells and CT26 cells *in vitro* and suppressed growth of CT26 tumours in the subaxilliary region in Balb/c mice *in vivo*. Cell-cycle arrest accompanied these observations. Expression of the nuclear transfer factor β-catenin and it translocation to the nucleus were also affected and the expression of its associated signal proteins Axin2 and c-Myb were increased and decreased, respectively. We demonstrate that PARP10 promotes proliferation of those colorectal carcinoma cells which express significant levels of PARP10. This promotion is suppressed when the enzymatic activity is inhibited. β-Catenin is likely to be the mediator of the antiproliferative effect.

Keywords: PARP10, β-catenin, colorectal carcinoma, proliferation

[#]These authors contributed equally to this work and should be considered co-first authors.

INTRODUCTION

Poly(ADP-ribose) polymerase-10 (PARP10 / ARTD10) is a member of PARP family which performs mono-ADP-ribosyl (MAR) transferase activity. It was originally identified as a

MYC-interacting protein and can mono(ADP-ribosyl)ate itself and core histones [1]. It has subsequently been reported to act on various cellular processes [2], including controlling cell apoptosis [3], neoplastic proliferation [4], tumor metastasis [5], and modulation of mitochondrial function [6]. PARP10 is present both in the nucleolus and the cytoplasm [7]. The nucleolar PARP10 has been reported to promote the proliferation of tumor cells [4] through involvement in the repair of DNA damage [8] and alteration of the cell cycle [9]. On the other hand, PARP10 could mono(ADP-ribosyl)ate a signaling protein that functionally adjusts proliferation by regulating the nuclear translocation protein β-catenin [10, 11].

Accumulating evidence draws our attention as to whether PARP10 has a regulatory role on proliferation of colorectal carcinoma. In the present study, we selected CRC cell lines with significantly positive PARP10 expression and applied a PARP10-selective inhibitor to investigate the influence of PARP10 on the proliferation of these CRC cells *in vitro* and *in vivo*. We have also explored, in part, the relevant signaling pathways involved.

EXPERIMENTAL

CRC cell lines and the PARP10-selective inhibitor. LoVo cells and SW480 cells were kindly provided by Professor WeiXue Tang of Chongqing Medical University. CT26 cells were generous provided by Professor YuQuan Wei of Sichuan University. LoVo cells were cultured in DMEM (Hyclone) supplemented with 10% FBS (Hyclone) and 1% penicillin/streptomycin (Byotime, Shanghai, China). CT26 cells and SW480 cells were cultured in RPMI-1640 (Hyclone) containing 10% fetal bovine serum and 1% penicillin/streptomycin and incubated under 5% CO_2 at 37°C. The PARP10-selective inhibitor 3-(*Z*-4-methylaminomethoxy-4-oxobutenoylamino)-benzamide was generously provided by Professor Mikael Elofsson (Umeå University). This inhibitor was identified from a series of twenty-six analogs designed as inhibitors of PARP10, ARTD8 and ARTD7 (**Figure 1**) [12]. The inhibitor was dissolved with DMSO (Sigma, USA) and prepared in RPMI-1640 medium at final concentrations of 0.5 μM to 4 μM and stored at 4°C in the dark.
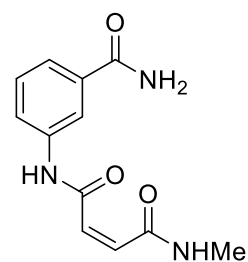

Fig. 1. Structure of the PARP10-selective inhibitor 3-(*Z*-4-methyl-aminomethoxy-4- oxobutenoyl-amino)benzamide.

Detection of expression of PARP10 in CRC cell lines by immunofluorescence. The expressions of PARP10 in CT26 cells, LoVo cells and SW480 cells were detected with an immunofluorescence assay. Cells were seeded onto slides in 24-well plates, incubated overnight at 37°C, fixed for 15 min with 4% paraformaldehyde, permeated for 20 min with 0.5% Triton and blocked for 30 min with goat serum at room temperature. PARP10 antibody (Santa Cruz, 1:20) was added to each well and cultured at 4°C overnight in the dark. After incubation with rabbit anti-goat IgG FITC (ZSGB-Bio) for 1.0 h at 37°C and DAPI for 5 min to stain the nuclei, the expression level and distribution of PARP10 were observed under a laser scanning confocal microscope (Leica TCS SP2, Leica Microsystems GmbH, Germany). The "laser power" and "PMT" were ensured to be consistent during detection of each cell lines and the fluorescence intensity of ten cells in each cell line were read. The mean was the average fluorescence intensity for each cell line. The experiments were performed in triplicate.

Detection of proliferation of CT26 cells, LoVo cells and SW480 cells *in vitro* using the CCK-8 assay. Cell proliferation was detected with CCK-8 kit (Byotime). CT26 cells (5×10^3), LoVo cells (5×10^3) and SW480 cells (5×10^3) in logarithmic phase were seeded into 96-well plates and incubated at 37°C under 5% CO_2 for 24 h. To the wells was added the PARP10 inhibitor at concentrations of 0.1 μM, 0.2 μM, 0.5 μM, 2.0 μM and 4.0 μM. Cells without PARP10 inhibitor were set as a control group and culture medium was used as the blank control. To determine the time-course of inhibition proliferation, CT26 cells and LoVo cells were treated with PARP10 inhibitor (0.5 μM) for 24 h, 48 h, 72 h, 96 h and 120 h. CCK-8 reagent (10 μL) was added to each well and incubated at 37°C for 1 h. Cell viability was measured at 450 nm using a microplate reader (Bio-Tek, Hercules, CA, USA) and represented by the optical density (OD). Five duplicate wells were set in each test and tests were repeated thrice.

Detection by flow cytometry of the influence of PARP10 on the cell cycle of CT26 cells. CT26 cells (1×10^4) of each group were collected, washed twice with PBS, suspended in the culture medium and centrifuged at 1000 rpm for 5 min. The cells were then washed with 70% ethanol, centrifuged at 1000 rpm for 5 min and subjected to flow cytometry (FACS Vantage SE, Becton Dickinson and Company, Franklin Lakes, NJ, USA). The proliferation index (PI) was measured according to: PI = (G2+S)/(G1+ G2+S). Tests were repeated thrice.

Animal studies：detection of the growth in CT26 cell tumors transplanted into Balb/c mice. All murine studies complied with the requirements of the Ethics Committee of Chongqing

Medical University and all necessary licenses were in place. Eight Balb/c male mice (Chongqing Medical University Laboratory Animal Center, Chongqing, China, 6-8 weeks old, 22-25 g, standard diet and water ad libitum) were randomly divided into a PARP10-inhibitor group and a control group. CT26 cells (2×10^6) were inoculated into their right armpits. From the eighth day after inoculation, the experimental group were injected intraperitoneally with the PARP10-selective inhibitor (2.0 mg Kg^{-1} dissolved in 200 μL normal saline) once a day and the control group were injected with normal saline (200 μL). The mice were sacrificed on the fourteenth day and the neoplasms were harvested. The weights and volumes of the transplanted tumors were measured. The volumes were calculated after the formula V = ab^2/2 (a, the longest diameter; b, the shortest diameter).

Detection of potential associated cell signal proteins in CT26 cells *in vitro* and *in vivo* with Western blot analysis. CT26 cells were cultured with or without PARP10-selective inhibitor (0.5 μM) for 72 h. They were then washed twice with ice-cold PBS and collected. The total cell proteins and nuclear proteins were extracted with nuclear and cytoplasm extraction reagents (Pierce). The concentrations of protein were evaluated with BCA protein assay kit (Byotime). Proteins (20 μg) were loaded on 8% polyacrylamide gels, separated by electrophoresis and transferred to polyvinylidene fluoride membrane (AmershamTM HybondTM, GE Healthcare Life Science). The membranes were then blocked with 5% non-fat milk for 2 h at room temperature and incubated with β-catenin (Cell Signaling, 1:1,000), Axin2 (Proteintech, 1:200), c-Myb (Proteintech, 1:500), Lamin B1 (Proteintech, 1:1,000) and β-Actin (Ding Guo, 1:1,000) overnight at 4°C. Then the membranes were washed twice with TBST and incubated with appropriate secondary antibodies (peroxidase-conjugated anti-rabbit, 1:1,000 or mouse immunoglobulin G, 1:1,000) for 2 h at room temperature. After being washed thrice with TBST, the membranes were visualized with BeyoECL Plus (Beyotime) and exposed to the gel formatter (Bio-Rad, CA, USA). The blots were analyzed with Quantity One Software (Bio-Rad). All experiments were performed in triplicate.

Statistical analysis. All quantitative data are reported as mean ± standard deviation (SD). Statistical analysis was performed by one-way ANOVA test or a student's t-test with the SPSS 19.0 statistical software. P-value <0.05 indicates a statistically significant difference.
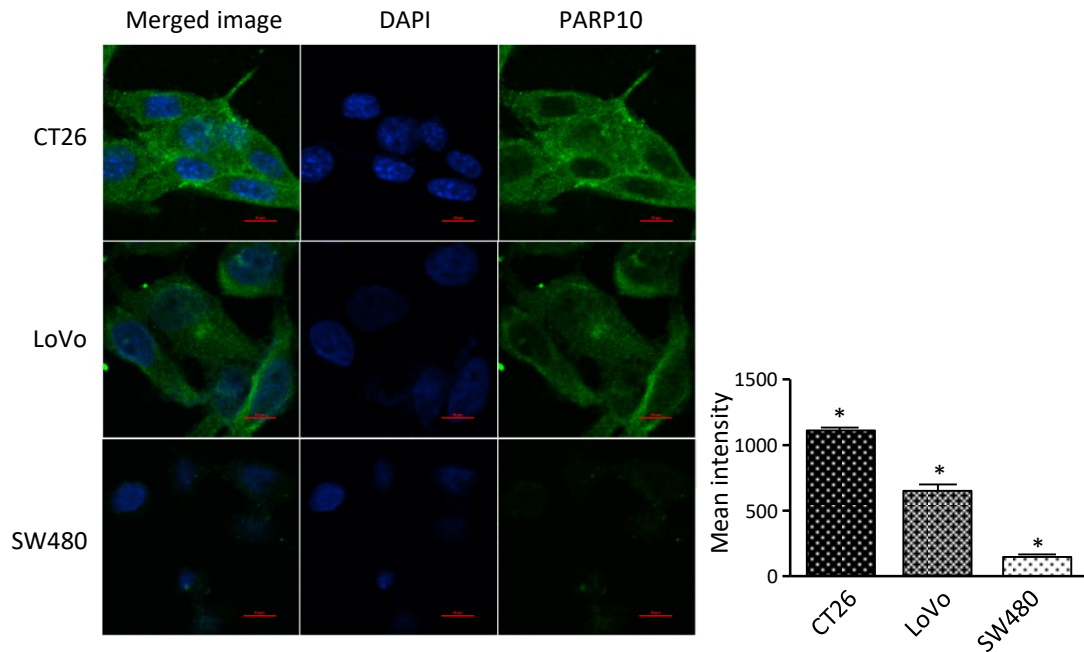
Fig. 2. Expression of PARP10 in different CRC cell lines. B, PARP10 expression in SW480 cells is faint to almost negative but is significantly positive in CT26 cells and LoVo cells. The positive staining was mainly located in the cytoplasm in both CT26 cells and LoVo cells. Meanwhile, some nuclei stained positively. **B**, The same "laser power" and "PMT" were set for the three cell lines. The fluorescence mean intensity of CT26 cells and Lovo cells significantly exceeded that of SW480 cells. (*P<0.001).

RESULTS

PARP10 positively expresses in two CRC cell lines

The expression of PARP10 differed in the three cells lines. The expression of PARP10 in SW480 was very weak, almost non-existent. However, it was expressed strongly in CT26 cells and LoVo cells, with statistically significant differences in the fluorescence mean intensity (P<0.001). Most of the positive-staining signal was located in cytoplasm but a few nuclei were also positively stained **(Figure 2)**.

Inhibition of PARP10 enzymatic activity suppresses the proliferation of CT26 cells and LoVo cells **in vitro**

A clear inhibitory effect on proliferation was observed when CT26 cells were cultured with different concentrations of PARP10 inhibitor for 72 h. There statistically differences between PARP10-inhibitor group and control group (P<0.05), except at 0.1 μM concentration of inhibitor (P>0.05). The intensity of the inhibition of proliferation become more apparent with increasing
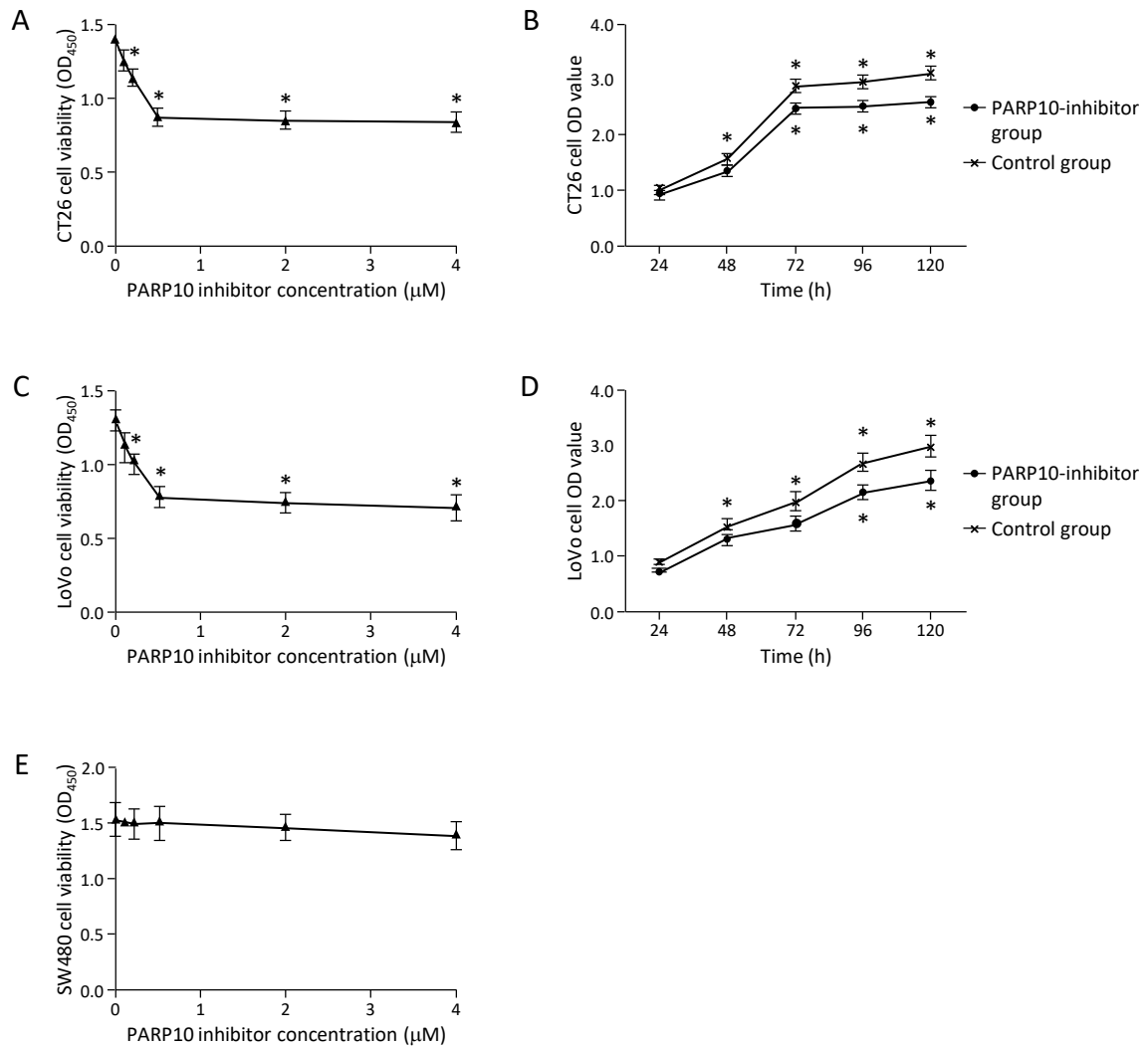
Fig. 3. Influence of PARP10 on the proliferation of CT26 cells; the cell viability was detected with the CCK-8 assay. **A**, CT26 cells were incubated with the PARP10-selective inhibitor (0.1 μM, 0.2 μM, 0.5 μM, 2.0 μM,d 4.0 μM) for 72 h, showing significant dosage-dependent correlation. Satisfactory effects were seen at 0.5 μM and higher concentrations. Values are expressed as mean ± SD (*P<0.05). **B**, CT26 cells were treated with PARP10 inhibitor for 24 h, 48 h, 72 h, 96 h and 120 h. The inhibitory effect showed significant time-dependence. Data are expressed as the mean ± SD (*P<0.05,**P <0.01). **C**, LoVo cells were incubated with the PARP10-selective inhibitor (0.1 μM, 0.2 μM, 0.5 μM, 2.0 μM, 4.0 μM) for 72 h, leading to significant dose-dependence. Satisfactory effects were seen at 0.5 μM and higher concentrations. Values are expressed as mean ± SD (*P<0.05). **D**, LoVo cells were treated with the PARP10-selective inhibitor for 24 h, 48 h, 72 h, 96 h and 120 h. The inhibitory effect showed significant time-dependence. Data are expressed as the mean ± SD (*P<0.05, **P<0.01). **E**, SW480 cells were incubated with the PARP10-selective inhibitor (0.1 μM, 0.2 μM, 0.5 μM, 2.0 μM, 4.0 μM) for 72 h; no statistically significant inhibitory effect was observed at all treatment concentrations (P>0.05).

concentrations of inhibitor, showing a significant dose-dependent relationship (P<0.05) (**Figure**
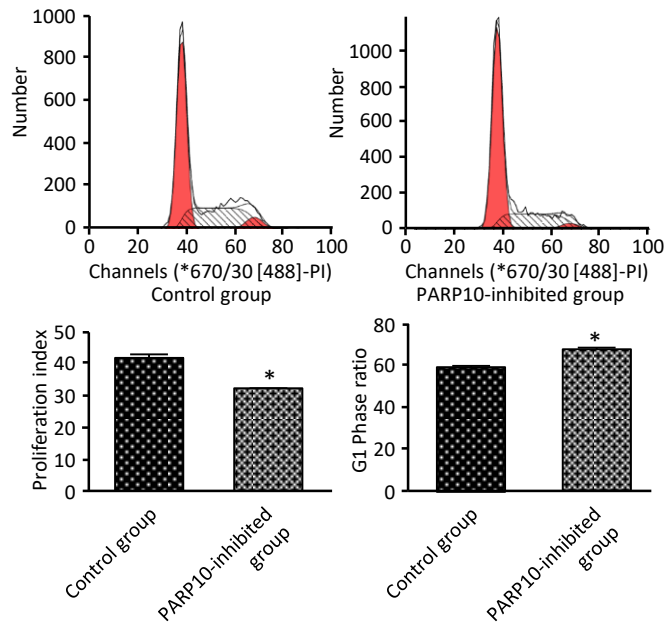
Figure 4: The G1 phase percentage in CT26 cells is significantly upgraded in the PARP10-inhibited group compared with the control group (*P<0.001). PI ratio in the PARP10-inhibited group decreased significantly compared with the control group (*P<0.001).

3A). A significant time-effect was also observed when CT26 cells were cultured with 0.5 μM PARP10-selective inhibitor for different incubation times (P<0.05) (**Figure 3B**). The results in LoVo cells were consistent with those in CT26 cells (P<0.05) (**Figure 3C,D**). On the contrary, different concentrations of PARP10-selective inhibitor failed to inhibit proliferation of SW480 cells significantly; this cell line has intrinsically low levels of PARP10. This supports the selectivity of the PARP10-selective inhibitor (P>0.05) (**Figure 3E**). In the light of these data, a treatment concentration of 0.5 μM and a treatment time of 72 h were selected for subsequent experiments.

Inhibition of PARP10 enzymatic activity blocks cell cycle of CT26 cells and LoVo cells by increasing the G1 phase ratio

The percentage of CT26 cells in G1 phase rose from 58.1 ± 1.1% to 67.4 ± 0.2% when PARP10 was inhibited (P<0.001). By contrast, PI decreased significantly in the PARP10-inhibitor group compared with the control group (P<0.001), corresponding to a decrease in proliferation rate of CT26 cells upon inhibition of PARP10 (**Figure 4**).

Inhibition of PARP10 enzymatic activity suppresses growth of CT26 subcutaneous tumors in Balb/c mice

The volume and weight of CT26 cell tumors subcutaneously transplanted in Balb/c mice significantly decreased in the PARP10-inhibitor group, compared to the control group (P<0.001) (**Figure 5** and **Table 1**), indicating that the effect of inhibition of PARP10 on proliferation of CT26 cells is consistent *in vitro* and *in vivo*.
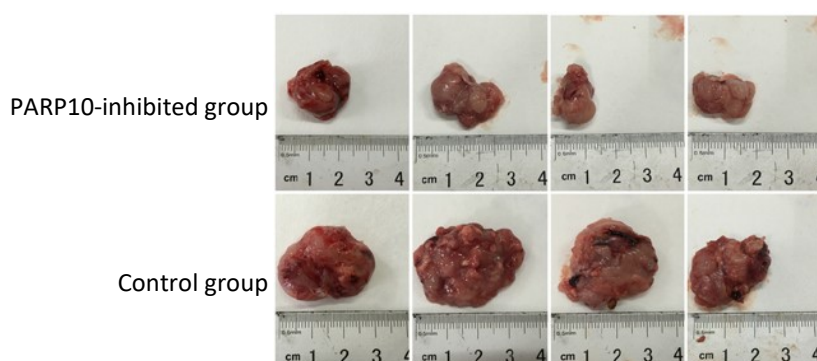

Figure 5: Effect of PARP10 on the growth of CT26 cell subcutaneous tumors in the armpit of Balb/c mice. The volumes of the tumors in the treated group are clearly smaller than those of the control group.

Inhibition of PARP10 enzymatic activity downregulates expression and nuclear transposition of β-catenin

Table 1. The volume and weight of CT26 tumours transplanted into Balb/c mice are significantly decreased in the group treated with the PARP10-selective inhibitor, compared to the control group.

	Volume (mL)	Weight (g)
Treated	3.33 ± 1.13	1.94 ± 0.53
Control	4.93 ± 1.03	2.16 ± 0.67
P	$<0.001^{**}$	$<0.001^{**}$
** One-way ANOVA		

Firstly, we detected the expression of β-catenin in CT26 cells. The Western blot showed that, when PARP10 was inhibited, the expression of β-catenin significantly decreased, compared with the control group both in whole cells and in cell nuclei (P<0.05) (**Figure 6**). This reveals that inhibition of PARP10 reduces both the total intracellular β-catenin and the entry of β-catenin into the nucleus. To translate this effect into the role of PARP10 *in vivo*, we assessed the expression of β-catenin in CT26 tumors subcutaneous transplanted in Balb/c mice. The results are consistent with those of *in vitro* experiments; when PARP10 activity was suppressed, the expression of β-catenin was significantly down-regulated compared with the control group, both in whole tumor cells and in tumor cell nuclei (P<0.05) (**Figure 7**).
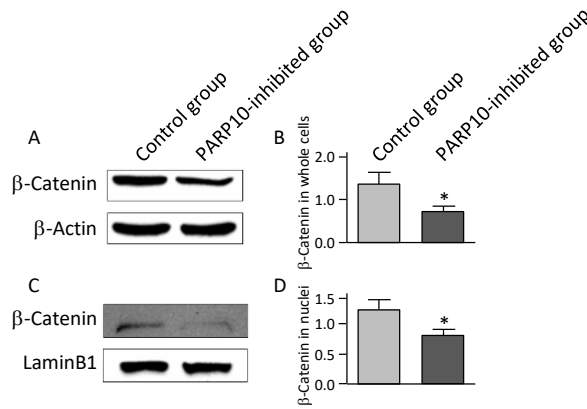
Figure 6: Expression of β-catenin. After 72 h of treatment with the PARP10-selective inhibitor, Western blot analysis identified the expression of β-catenin in CT26 cells. β-Actin and LaminB1 were used as controls of total protein and nuclear protein, respectively. **A** and **B**: Inhibition of PARP10 down-regulated the total amount of β-catenin protein in CT26 cells; data are expressed as the mean ± SD (*P< 0.05). **C** and **D**: Inhibition of PARP10 down-regulated the amount of nuclear β-catenin protein; data are expressed as the mean ± SD (*P< 0.05).
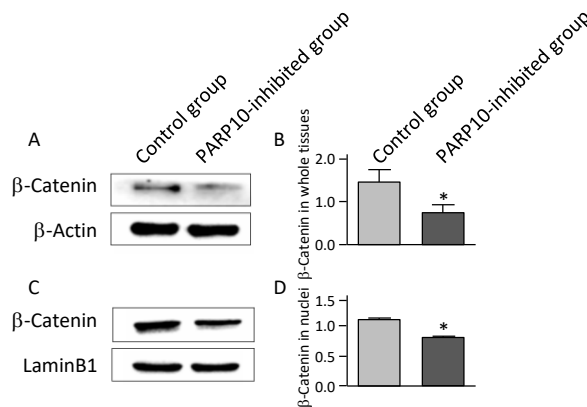

Figure 7: Expression of β-catenin in CT26 tumors *in vivo*. After injecting Balb/c mice with the PARP10-selective inhibitor (2.0 mg Kg^{-1}) or 0.9% normal saline intraperitoneally for 1 week, expression of β-catenin protein in the CT26 transplanted tumor was analyzed by Western blot. β-Actin and LaminB1 were used as controls of total protein and nuclear protein, respectively. **A** and **B**: Inhibition of PARP10 down-regulated the total amount of β-catenin protein; data are expressed as the mean ± SD (*P< 0.05). **C** and **D**: Inhibition of PARP10 down-regulated the amount of β-catenin protein in the nucleus; data are expressed as the mean ± SD (*p< 0.01).

Inhibition of PARP10 enzymatic activity changes the protein expression of Axin2 and c-Myb

Axin2 and c-Myb are both cell signaling proteins, which are closely functionally related to β-catenin and have a close connection with cell proliferation. As the results shows, when PARP10 is inhibited, expression of Axin2 was significantly increased, while that of nuclear c-Myb decreased markedly (P<0.05) (**Figure 8**).
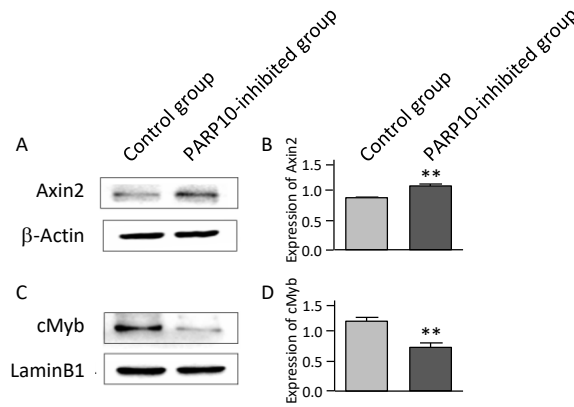
Figure 8: Expression of Axin2 and c-Myb. After treatment with 0.5 μM PARP10 inhibitor for 72 h, the level of Axin2 protein in CT26 cells and c-Myb protein in CT26 cell nucleus were measured by Western blot analysis. β-Actin and LaminB1 were used as controls for total cellular protein and nuclear protein, respectively. **A** and **B**: Inhibition of PARP10 up-regulated the expression of Axin2 protein; data are expressed as the mean ± SD (**p< 0.01). **C** and **D**: Inhibition of PARP10 down-regulated the expression of c-Myb protein compared with the control group; data are expressed as the mean ± SD (**p< 0.01).

DISCUSSION

Several biological functions of the recently discovered mono-(ADP-ribosyl)transferase, PARP10, have been uncovered; these include influencing virus replication [13,14], and regulation of proliferation, apoptosis, metastasis and cycling in eukaryotic cells [2]. It is reported that knockdown of PARP10 in HeLa cells results in inhibition of growth and reduced tumorigenesis. Its overexpression in non-transformed RPE-1 cells alleviates their sensitivity to replication stress, fosters the restart of stalled replication forks and results in formation of tumors in a mouse xenograft model [4]. Silencing PARP10 decreases the proliferation rate in MCF7 cells, while increasing the expression of PARP10 can promote proliferation [6]. However, the effect of PARP10 on the proliferation of different types of colorectal carcinoma (CRC) cells is not clear.

We explored the influence of PARP10 activity on the proliferation of three CRC cell lines, LoVo, CT26 and SW480. PARP10 is expressed in both nucleoli and cytoplasm in LoVo cells and in CT26 cells but is barely expressed at all in SW480 cells. The pattern of expression is consistent with previous reports [7]. The inhibition of PARP10 enzymatic activity resulted in a statistically significant decrease of proliferation rate in both LoVo and CT26 cells and this decrease is related to both concentration and time. This makes it reasonable to suggest that CRC cells which are positive in expression of PARP10 may be sensitive to inhibition of the enzymatic

activity of PARP10. To translate the effect of PARP10 into tumors *in vivo*, we established a model of CT26 tumors transplanted subcutaneously in the axillae of Balb/c mice. The growth of these tumors was significantly suppressed in the PARP10 inhibitor group, suggesting that the effect of PARP10 in promoting proliferation of CRC cells is repeatable *in vivo*. Furthermore, significantly increased G1 phase ratio and decreased PI have been observed in CT26 cells when PARP10 is inhibited, providing a reasonable explanation for the previously observed decreased proliferation of CT26 cells when PARP10 enzymatic activity is inhibited.

β-Catenin is a second messenger which acts as a transcription factor to promote proliferation [15,16]. It is also a downstream signaling protein of target protein(s) regulated by PARP10 [11]. To search for the proliferation-regulating nuclear transcriptional proteins that PARP10 might affect, we chose to detect β-catenin. When we selectively inhibited PARP10, expression of β-catenin was significantly downregulated in both CT26 cells and CT26 transplanted tumors in Balb/c mice, indicating that total β-catenin and nuclear β-catenin in CT26 cells both decreased, *in vitro* and *in vivo*, strongly suggesting a role of PARP10 in the regulation of β-catenin.

GSK3β is upstream signaling protein of β-catenin in Wnt pathway, participating in formation of the β-catenin degradation complex and degradation of β-catenin through phosphorylation. When there is no Wnt signal, β-catenin combines with GSK3β, Axin, APC and Fzd to form a complex and are phosphorylated by GSK3β or hydrolyzed by autophagy or the ubiquitin-proteasome system (UPS) [11]. When the Wnt pathway is activated, the GSK3β/Axin/APC complex disintegrates and β-catenin cannot not be degraded. In a recent report, GSK3β was identified as a substrate for PARP10-catalyzed mono(ADP-ribosyl)ation in a protein microarray screen *in vitro*; its kinase activity is inhibited when it is mono(ADP-ribosyl)ated by PARP10 [7, 17]. Thus we speculate that PARP10 may inhibit the degradation of β-catenin by abolishing the kinase activity of GSK3β by mono(ADP-ribosyl)ing the latter. When PARP10 is inhibited, the kinase activity of GSK3β recovers and β-catenin can be degraded and its abundance in cells decreases. How this regulation of β-catenin by PARP10 through GSK3β also applies in PARP10-positive CRC cells needs to be further verified.

β-Catenin translocates into the nucleus through nucleoporin 62 (NUP62), replacing the CoR, binds to transcription factors such as TCF/LEF, HIF-1α and TBX5, and activates transcription of proliferation-related downstream signal proteins including Axin2 and c-Myb [15,16]. To confirm whether changes in nuclear translocation levels of β-catenin alters the expression of downstream

signaling pathway proteins, the expression of a transcriptional protein that is under its regulation, c-Myb, was measured. C-Myb has been reported to interact with a large number of potential regulators of its activity, including protein kinases, cell cycle regulators and transcription factors, It acts as an oncogenic protein, is overexpressed in tumors such as CRC and promotes proliferation of tumor cells by activating the genes which responsible for G/S phase and G/M phase transition [18-20]. As observed in this study, the amount of c-Myb protein in the nucleus declined in CT26 cells where PARP-10 enzymatic activity was inhibited, indicating that the expression and functional changes of β-catenin bring about downstream effects. It is worth noting that, if we infer the influence of changes in the level of c-Myb protein on the cell cycle distribution of the PARP10-inhibited CT26 cells, it will be consistent with the G1 phase block we have detected. Does the reduced expression of β-catenin and its nuclear translocation influence proliferation by through c-Myb in PARP10-inhibited CT26 cells? Further verification is needed.

At the same time, abnormally high expression of Axin2 is found in tumors which have functional defects in β-catenin [21]. It effectively promotes the degradation of β-catenin by assembling the GSK3β/Axin/APC/Fzd multiprotein complex which destroys β-catenin [22,23]. In the present study, expression of Axin2 is up-regulated in the PARP10-inhibited group in comparison to the control group. Thus we infer that, in PARP10-inhibited CT26 cells, decreased nuclear translocation levels of b-catenin leads to up-regulated levels of Axin2. Then the elevated Axin2 acts as a feedback repressor, contributing to strengthen the effect of decrease of β-catenin and further promoting the down-regulation of expression and function of β-catenin. Currently, attempts to increase expression of Axin1/2, thereby down-regulating the constitutive stabilization of β-catenin, shows therapeutic activity in CRC [24,25]. So β-catenin is very likely to regulate the expression of Axin-2, and then enhances its down-regulation effect through the Axin-2 feedback loop in CRC cells with positive expression of PARP10.

The subcellular locale where PARP10 mono(ADP-ribosyl)ates GSK3β is the cytoplasm. PARP10 is shown to be largely present in the cytoplasm in LoVo cells and in CT26 cells in our present study. This gives us reason to speculate that the cytoplasm PARP10 regulates the proliferation of CRC cells by regulating the expression and function of β-catenin [7,10,17].

The PARP10 subgroup located in the nucleoli has also been reported to play a direct and effective working role in cellular proliferation. PARP10 serves as a binding partner for PCNA to

protect genomic stability and is required for translation and DNA synthesis [26,27]. Down-expression of PARP10 leads to delayed G1 progression and concomitant cell death in HeLa cells [9]. We have observed increased G1 phase cells ratio and decreased PI ratio in the PARP10-inhibited CRC cells. The trend is consistent with existing reports, strongly supporting this mechanism of regulation of proliferation by nucleolar PARP10. We speculate strongly that PARP10, possibly recruited by PTEN in the nucleoli of cells, binds with PTEN to the damaged sites in DNA, stimulates the replication and repair mechanism, regulates the cell cycle, and then affects the proliferation of CRC cells [4,26].

It should be mentioned is the effect of PARP10 on the biological behavior of tumor cells is never a simple and one-way trend [3,5,8,28]. More detailed studies on the mechanism of PARP10's proliferative regulation in CRC cells may help for explore the roles of PARP10. Whether the regulation of PARP10 on the proliferation of CRC cells can be extended to other types of tumor cells also has research value.

CONCLUSIONS

We have observed that PARP10 promotes proliferation of those CRC cells in which significant levels of PARP10 are present. Conversely, inhibition of its enzymatic activity nullifies this activation. We also demonstrate that nuclear translocation protein β-catenin participates in this function.

ACKNOWLEDGMENTS

Chongqing Medical University (JC201509) and the Yingyao Project of Basic Medical College, Chongqing Medical University (JCYY201701).

CONFLICTS OF INTEREST

The authors declare no conflict of interest.

ETHICAL STATEMENTS

All applicable international, national, and/or institutional guidelines for the care and use of animals were followed in this study. This article does not contain any studies involving human participants performed by any of the authors.

REFERENCES

1. Kleine H., Poreba E., Lesniewicz K., Hassa P. O., Hottiger M. O., Litchfield D. W., Shilton B. H., Lüscher B. (2008) Substrate-assisted catalysis by PARP10 limits its activity to mono-ADP-ribosylation. *Mol. Cell.* **32**, 57–69.

2. Bütepage M., Eckei L., Verheugd P., Lüscher B. (2015) Intracellular mono-ADP-ribosylation in signaling and disease. *Cells* **4**, 569-595.

3. Herzog N., Hartkamp J. D., Verheugd P., Treude F., Forst A. H., Feijs K. L. H., Lippok B. E., Kremmer E., Kleine H., Lüscher B. (2013) Caspase-dependent cleavage of the mono-ADP-ribosyltransferase ARTD10 interferes with its pro-apoptotic function. *FEBS J.* **280**, 1330-1343.

4. Schleicher E. M., Galvan A. M., Imamura-Kawasawa. Y., Moldovan G.-L., Nicolae C. M. (2018) PARP10 promotes cellular proliferation and tumorigenesis by alleviating replication stress. *Nucleic Acids Res.* **46**, 8908-8916.

5. Zhao Y., Hu X., Wei L., Song D., Wang J., You L., Saiyin H., Li Z., Yu W., Yu L., Ding J., Wu J. (2018) PARP10 suppresses tumor metastasis through regulation of Aurora A activity. *Oncogene* **37**, 2921-2935.

6. Márton J., Fodor T., Nagy L., Vida A., Kis G., Brunyánszki A., Antal M., Lüscher B., Bai P. (2018) PARP10 (ARTD10) modulates mitochondrial function. *PLoS One.* **13**, e0187789.

7. Kleine H., Herrmann A., Lamark T., Forst A. H., Verheugd P., Lüscher-Firzlaff. J., Lippok B., Feijs K. L., Herzog N., Kremmer E., Johansen T., Muller-Newen G., Lüscher B. (2012) Dynamic subcellular localization of the mono-ADP-ribosyltransferase ARTD10 and interaction with the ubiquitin receptor p62. *Cell. Commun. Signal* **10**, 10-28.

8. Kaufmann M., Feijs K. L., Lüscher B. (2015) Function and regulation of the mono-ADP-ribosyltransferase ARTD10. *Curr. Topics Microbiol. Immunol.* **384**, 167-188.

9. Chou H. Y., Chou H. T., Lee S. C. (2006) CDK-dependent activation of poly(ADP-ribose) polymerase member 10 (PARP10). *J. Biol. Chem.* **281**, 15201-15207.

10. Feijs K. L., Kleine H., Braczynski A., Forst A. H., Herzog N., Verheugd P., Linzen U., Kremmer E., Lüscher B. (2013) ARTD10 substrate identification on protein microarrays: regulation of GSK3beta by mono-ADP-ribosylation. *Cell. Commun. Signal* **11**, 11-15.

11. Wu D., Pan W. (2010) GSK3: a multifaceted kinase in Wnt signaling. *Trends Biochem. Sci.* **35**, 161-168.

12. Ekblad T., Lindgren A. E. G., Andersson C. D., Caraballo R., Thorsell A.-G., Karlberg T., Spjut S., Linusson A., Schüler H., Elofsson M. (2015) Towards small molecule inhibitors of mono-ADP-ribosyltransferases. *Eur. J. Med. Chem.* **95**, 546-551.

13. Atasheva S., Frolova E. I., Frolov I. (2014) Interferon-stimulated poly(ADP-ribose) polymerases are potent inhibitors of cellular translation and virus replication. *J Virol.* **88**, 2116-2130.

14. Yu M., Zhang C., Yang Y., Yang Z., Zhao L., Xu L., Wang R., Zhou X., Huang P. (2011) The interaction between the PARP10 protein and the NS1 protein of H5N1 AIV and its effect on virus replication. *Virol. J.* **8**, 546.

15. Majidinia M. A. J., Jahanban-Esfahlani R., Yousefi B. (2018) The roles of Wnt/β-catenin pathway in tissue development and regenerative medicine. *J. Cell. Physiol*. **233,** 5598-5612.

16. Yang X., Gu Q., Lin L., Li S., Zhong S., Li Q., Cui Z. (2015) Nucleoporin 62-like protein activates canonical Wnt signaling through facilitating the nuclear import of β-catenin in zebrafish. *Mol. Cell. Biol.* **35,** 1110-1124.

17. Yu M., Schreek S., Cerni C., Schamberger C., Lesniewicz K., Poreba E., Vervoorts J., Walsemann G., Grotzinger J., Kremmer E., Mehraein Y., Mertsching J., Kraft R., Austen M., Lüscher-Firzlaff J., Lüscher B. (2005) PARP-10, a novel Myc-interacting protein with poly(ADP-ribose) polymerase activity, inhibits transformation. *Oncogene.* **24**, 1982-1993.

18. Biroccio A., Benassi B., D'Agnano I., D'Angelo C., Buglioni S., Mottolese M., Ricciotti A., Citro G., Cosimelli M., Ramsay R. G., Calabretta B., Zupi G. (2001) c-Myb and Bcl-x overexpression predicts poor prognosis in colorectal cancer: clinical and experimental findings. *Am J Pathol.* **158**, 1289-1299.

19. Ramsay R. G., Gonda T. J. (2008) MYB function in normal and cancer cells. *Nature Rev. Cancer* **8**, 523-534.

20. McCubrey J. A., Steelman L. S., Bertrand F. E., Davis N. M., Abrams S. L., Montalto G., D'Assoro A. B., Libra M., Nicoletti F., Maestro R., Basecke J., Cocco L., Cervello M., Martelli A. M. (2014) Multifaceted roles of GSK-3 and Wnt/β-catenin in hematopoiesis and leukemogenesis: opportunities for therapeutic intervention. *Leukemia* **28**, 15-33.

21. Leung J. Y., Kolligs F. T., Wu R., Zhai Y., Kuick R., Hanash S., Cho K. R., Fearon E. R. (2002) Activation of AXIN2 expression by β-catenin-T cell factor. A feedback repressor pathway regulating Wnt signaling. *J. Biol. Chem.* **277**, 21657-21665.

22. Herbst A., Jurinovic J., Krebs S.., Thieme S. E.., Blum H., Göke B., Kolligs F. T.. (2014) Comprehensive analysis of β-catenin target genes in colorectal carcinoma cell lines with deregulated Wnt/β-catenin signaling. *BMC Genomics* **15:** 74.

23. Wu Z. Q., Brabletz T., Fearon E., Willis A. L., Hu C. Y., Li X. Y., Weiss S. J. (2012) Canonical Wnt suppressor, Axin2, promotes colon carcinoma oncogenic activity. *Proc Natl Acad Sci U S A.* **109**, 11312-11317.

24. Nathubhai A., T. Haikarainen T., Koivunen J., Murthy S., Koumanov F., Lloyd M. D., Holman G. D., Pihlajaniemi T., Tosh D., Lehtiö L., Threadgill M. D. (2017) Highly potent and isoform selective dual site binding tankyrase/Wnt signaling inhibitors that increase cellular glucose uptake and have antiproliferative activity. *J. Med. Chem.* **60**, 814-820.

25. Jeong W. J., Ro E. J., Choi K. Y. (2018) Interaction between Wnt/β-catenin and RAS-ERK pathways and an anti-cancer strategy via degradations of β-catenin and RAS by targeting the Wnt/β-catenin pathway. *NPJ Precis Oncol.* **2**, 5.

26. Nicolae C. M., Aho E. R., Vlahos A. H., Choe K. N., De S., Karras G. I., Moldovan G. L. (2014) The ADP-ribosyltransferase PARP10/ARTD10 interacts with proliferating cell nuclear antigen (PCNA) and is required for DNA damage tolerance. *J. Biol. Chem.* **289**, 13627-13637.

27. Shahrour M. A., Nicolae C. M., Edvardson S., Ashhab M., Galvan A. M., Constantin D., Abu-Libdeh B., Moldovan G. L., Elpeleg O. (2016) PARP10 deficiency manifests by severe developmental delay and DNA repair defect. *Neurogenetics* **17**, 227-232.

28. Verheugd P., Forst A. H., Milke L., Herzog N., Feijs K. L., Kremmer E., Kleine H., Luscher B. (2013) Regulation of NF-κB signalling by the mono-ADP-ribosyltransferase ARTD10. *Nature Commun.* **4**, 1683.